

# Observation of the Epitaxial Satellite Phase in the Superconducting $\text{RuSr}_2\text{Eu}_{1.5}\text{Ce}_{0.5}\text{Cu}_2\text{O}_{10}$ Ceramic Samples

V. V. Petrykin,\* M. Osada, and M. Kakihana

*Materials and Structures Laboratory, Tokyo Institute of Technology, 4259 Nagatsuta, Midori, Yokohama 226-8503, Japan*

Y. Tanaka and H. Yasuoka

*Department of Applied Physics, National Defense Academy, 1-10-20 Hashirimizu, Yokosuka 239-8686, Japan*

Y. Ueki

*Application Technology Department, Hitachi Science Systems, 882 Ichige, Hitachinaka, Ibaraki 312-8504, Japan*

M. Abe

*Department of Physical Electronics, Tokyo Institute of Technology, 2-12-1 Ookayama, Tokyo 152-8552, Japan*

*Received March 17, 2003. Revised Manuscript Received August 20, 2003*

We have compared nonsuperconducting and superconducting ceramic samples of  $\text{RuSr}_2\text{Eu}_{1.5}\text{Ce}_{0.5}\text{Cu}_2\text{O}_{10}$  prepared by a polymerizable complex method using Raman spectroscopy and electron diffraction. The superconductivity in these ruthenocuprate samples was associated with ruthenium deficiency. It turned out that superconducting samples contain an epitaxial satellite phase having lattice parameters of  $\mathbf{a} = 3.8407\text{\AA}$ ,  $\mathbf{c} = 11.417\text{\AA}$  ( $\mathbf{a}/\mathbf{c} \approx 3$ ), whereas Raman spectra revealed the presence of carbonate groups, which coordinate metal ions in a manner similar to that in the superconducting carboxycuprates. Therefore, we speculate that the satellite phase is  $\text{EuSr}_2\text{Cu}_{3-x}(\text{CO}_3)_x\text{O}_{7+z}$  doped with Ru into Cu chain site and it might be responsible for superconductivity. The intergrowth of such a phase was confirmed by HREM.

## Introduction

The first syntheses of  $\text{RuSr}_2\text{LnCu}_2\text{O}_8$  (Ru-1212) and  $\text{RuSr}_2(\text{Ln}_{1-x}\text{Ce}_x)_2\text{Cu}_2\text{O}_{10}$  (Ru-1222) layer cuprates where Ln = Sm, Eu, and Gd have been reported by Bauernfeind et al.<sup>1</sup> The Ru-1212 member of Ru based cuprate series can be described as oxygen deficient triple perovskite isostructural to  $\text{LnBa}_2\text{Cu}_3\text{O}_7$  compounds in which CuO chains are replaced with the  $\text{RuO}_2$  layers. The  $\text{RuO}_6$  octahedra are slightly tilted to accommodate longer Ru oxygen bonds.<sup>2</sup> The oxygen sites in the  $\text{RuO}_2$  layer are fully occupied and there is no degree of freedom to adjust carrier concentration. Therefore as-prepared samples were semiconducting and after subsequent oxidation only a very small superconducting volume fraction could be found.<sup>1</sup> The structure of  $\text{RuSr}_2(\text{Ln}_{1-x}\text{Ce}_x)_2\text{Cu}_2\text{O}_{10}$  can be derived from Ru-1212 structure by replacement of the Ln layer with fluorite block  $(\text{Ln}_{1-x}\text{Ce}_x)_2\text{O}_2$ , which results in the shift of the adjacent perovskite block by  $(\mathbf{a} + \mathbf{b})/2$  and, consequently, in doubling of the unit cell along the  $c$ -axis.<sup>3</sup>  $\text{Ce}^{4+}$  doping

onto the  $\text{Ln}^{+3}$  site, as well as oxygen nonstoichiometry in the fluorite block, provides a convenient means to adjust carrier concentration. It was found that optimally doped compounds with  $x = 0.5\text{--}0.6$  became superconducting at  $T_C \sim 40\text{ K}$ .<sup>1</sup>

Felner and co-workers discovered that superconductivity in Ru-1222 coexists with ferromagnetism<sup>4</sup> where  $T_N = 180\text{ K}$  for Ln = Gd and  $T_N = 122\text{ K}$  for Ln = Eu were much higher than  $T_C$ . The magnetic susceptibility data and Mössbauer spectroscopy studies indicated that superconductivity might be confined to  $\text{CuO}_2$  planes, whereas the  $\text{RuO}_2$  layer is responsible for ferromagnetic properties. Coexistence of such mutually excluding phenomena triggered active studies of both Ru-1212 and Ru-1222 compounds. Soon Tallon et al.<sup>5</sup> reported that  $\text{RuSr}_2\text{GdCu}_2\text{O}_8$  also becomes ferromagnetic below 132 K, and after 7 d synthesis at 1060 °C one can obtain superconducting samples with zero resistivity at 21 K. Ferromagnetism and superconductivity seemed to be

(1) Bauernfeind, L.; Widder, W.; Braun, H. F. *Physica C* **1995**, *254*, 151.

(2) Chmaissem, O.; Jorgensen, J. D.; Shaked, H.; Dollar, P.; Tallon, J. L. *Phys. Rev. B* **2000**, *61*, 6401.

(3) Knee, C. S.; Rainford, B. D.; Weller, M. T. *J. Mater. Chem.* **2000**, *10*, 2445.

(4) Felner, I.; Asaf, U.; Levi, Y.; Millo, O. *Phys. Rev. B* **1997**, *55*, R3374.

(5) Tallon, J.; Bernhard, C.; Bowden, M.; Gilbert, P.; Stoto, T.; Pringle, D. *IEEE Trans. Appl. Supercond.* **1999**, *9*, 1696.

bulk properties according to their studies. The main conclusions achieved since then can be summarized as follows: (1) ceramic samples of both Ru-1212 and Ru-1222 exhibit ferromagnetic behavior ( $T_N(\text{RuSr}_2\text{GdCu}_2\text{O}_8) = 132 \text{ K}$ ,<sup>2,5,6</sup>  $T_N(\text{RuSr}_2(\text{Eu,Ce})_2\text{Cu}_2\text{O}_{10}) = 122 \text{ K}$ ,  $T_N(\text{RuSr}_2(\text{Gd,Ce})_2\text{Cu}_2\text{O}_{10}) = 180 \text{ K}$ <sup>3,4</sup>) and become superconducting at  $T_C \ll T_N$  ( $T_C(\text{Ru-1212}) = 20\text{--}35 \text{ K}$ ,<sup>2,5</sup> and  $T_C(\text{Ru-1222}) = 30\text{--}40 \text{ K}$ <sup>1,3,4</sup>); (2) the chemical composition of the principal phase is uniform within the accuracy and resolution of EDS;<sup>7</sup> (3) ferromagnetism and superconductivity coexist in space within resolution of magneto-optical imaging of  $\sim 10 \mu\text{m}$ ;<sup>8</sup> (4) despite the skepticism of physicists, ferromagnetic moment and superconducting coupling within same unit cells have been anticipated in computational studies;<sup>9,10</sup> (5) however careful analysis of magnetic and resistivity data of Ru-1212 and Ru-1222 allowed assuming that both compounds might not be uniform bulk superconductors, but ferromagnetism and superconductivity appear in different domains.<sup>11</sup>

Despite the fact that a lot of studies of the physical properties of Ru-1212 and Ru-1222 have been carried out, there is no clear understanding whether ferromagnetic and superconducting transitions do take place within the same unit cell, or if ferromagnetic and superconducting regions are separated in the space. Although both compounds are equally interesting for physicists, from the viewpoint of a chemist or a materials scientist, synthesis of Ru-1222 is the more challenging task because the optimal superconducting composition includes an additional component compared to Ru-1212; the synthesis usually requires higher temperature, which may indicate existence of the kinetic difficulties for phase formation; and in the required temperature range one should consider an interplay between copper valence necessary to form stable crystal and oxygen fugacity under given conditions.

Analysis of the described experimental conditions in the published studies helped conclude that Ru-1212 forms faster than Ru-1222 and at lower temperature; typical samples always contain impurities, and Ru-1212 samples are systematically of better quality than samples of Ru-1222. Unfortunately, most of the authors avoid presenting X-ray diffraction patterns. Therefore it is very difficult to compare studies carried out by different groups and difficult to conclude what is the primary obstacle for syntheses of single-phase samples. In other words, it might be a kinetic difficulty due to the poor homogeneity achieved in the conventional solid state reaction method (to the best of our knowledge nobody has tried to apply advanced synthesis techniques), or a compound with the idealized formula such as  $\text{RuSr}_2\text{Ln}_{1.5}\text{Ce}_{0.5}\text{Cu}_2\text{O}_{10}$  does not exist, and we are dealing with

the solid solution where Eu or Gd may enter the Sr site and the Ru site is shared also by Cu and Ce.<sup>12</sup> In the latter case, M-1222 phases are isostructural to Ru-1222 and become superconducting at  $T_C$  of 30–36 K depending on the composition!

Recently we have reported the preparation of high-quality  $\text{RuSr}_2\text{Eu}_{1.5}\text{Ce}_{0.5}\text{Cu}_2\text{O}_{10}$  samples using a variation of sol-gel technique – polymerizable complex method.<sup>13</sup> It turned out that single phase and nearly single-phase samples do not become superconducting even at liquid helium temperature, though they do show ferromagnetic behavior. Despite that resistivity changed its character in the region of the reported  $T_C$  values, there was no evidence of bulk superconductivity or large volume fraction of the superconducting phase even after oxygen annealing under elevated pressure. We noticed that phase composition of the superconducting samples described in the literature<sup>1,3,4</sup> looks similar to that of Ru deficient samples in our earlier experiments, when we did not control  $\text{RuO}_2$  vaporization from the pellet. The intentionally prepared Ru deficient samples have demonstrated superconductivity. We have therefore decided to clarify the difference between superconducting and nonsuperconducting Ru-1222 ceramics using electron microscopy and Raman spectroscopy—characterization techniques available in our group.

## Experimental Section

All samples for this report have been prepared as previously described<sup>13</sup> with minor modification of the solution processing step.  $\text{Eu}_2\text{O}_3$  (or  $\text{Gd}_2\text{O}_3$ ) preheated at 900 °C for 12 h was dissolved in 10 wt. % excess of nitric acid. Then ethylene glycol and citric acid were added and stirred till dissolution. Cerium acetate stock solution,  $\text{SrCO}_3$ , and basic copper carbonate  $\text{Cu}(\text{OH})_2 \cdot \text{CuCO}_3$  powders were added to the solution. All chemicals were of at least 99.9% purity obtained from commercial sources. Copper content in the basic copper carbonate and  $\text{Ce}^{3+}$  concentration in the cerium acetate stock solution were determined by chemical analysis prior to their use. The precursor solution was kept at 60 °C overnight to ensure complete dissolution of solids, then the pH was adjusted by  $\text{NH}_3(\text{aq})$  to 6; the temperature of the hot plate was set to 140 °C and kept for 24 h till the formation of brown viscous gel. Afterward, the temperature of the hot plate was set to 200 °C to evaporate the excess of ethylene glycol. The prepared dark hard gel was crushed and subjected to pyrolysis at 400 °C. The remained organics were oxidized at 600 °C in air for 2 h, and the thus-obtained powder was calcinated in dynamic vacuum ( $\sim 2$  Torr) to decompose carbonates at 840 °C for 12 h. The obtained precursor powder was mixed with the required amount of  $\text{RuO}_2$  (99.9% purity), pressed into pellets, and heat treated in the sealed crucible at 1060 °C under  $P_{\text{O}_2} = 1 \text{ atm}$  for 48 h with one intermediate grinding after 24 h. The pellets were put onto a MgO single crystal to prevent their interaction with the crucible during the synthesis.

The X-ray diffraction patterns of the prepared samples were collected in Bragg–Brentano configuration by a MacScience X-ray diffractometer with  $\text{Cu K}\alpha$  radiation in the step scanning mode with 5 s/step and  $\Delta 2\theta = 0.02^\circ$ . Lattice parameters were calculated by the least-squares method.

The dc-resistivity was measured by a conventional four-probe method. The electrodes were formed by applying a gold paste. The temperature of the sample decreased at the rate of 0.3 K/min. Magnetic susceptibility data were measured by SQUID MPMS-5.

(6) Tallon, J. L.; Bernhard, C.; Loram, J. W. *J. Low Temp. Phys.* **1999**, *117*, 823.

(7) Chu, C. W.; Xue, Y. Y.; Wang, Y. S.; Heilman, A. K.; Lorenz, B.; Meng, R. L.; Cmaidalka, J.; Dezaneti, L. M. *J. Supercond.* **2000**, *13*, 679.

(8) Chen, S. Y.; Shulman, J.; Wang, Y. S.; Cao, D. H.; Wang, C.; Chen, Q. Y.; Johansen, T. H.; Chu, W. K.; Chu, C. W. <http://arxiv.org/abs/cond-mat/0105510v1>.

(9) Nakamura, K.; Park, K. T.; Freeman, A. J.; Jorgensen, J. D. *Phys. Rev. B* **2000**, *63*, 024507-1.

(10) Shick, A. B.; Weht, R.; Pickett, W. E. *J. Supercond.* **2000**, *13*, 687.

(11) Xue, Y. Y.; Lorenz, B.; Baikalov, A.; Cao, D. H.; Li, Z. G.; Chu, C. W. *Phys. Rev. B* **2002**, *66*, 014503-1.

(12) Kopnin, E. M.; Kharlanov, A. L.; Bryntse, I.; Antipov, E. V. *Physica C* **1994**, *219*, 47.

(13) Petrykin, V. V.; Kakihana, M.; Tanaka, Y.; Yasuoka, H.; Abe, M.; Eriksson, S. *Physica C* **2002**, *378*, 47.

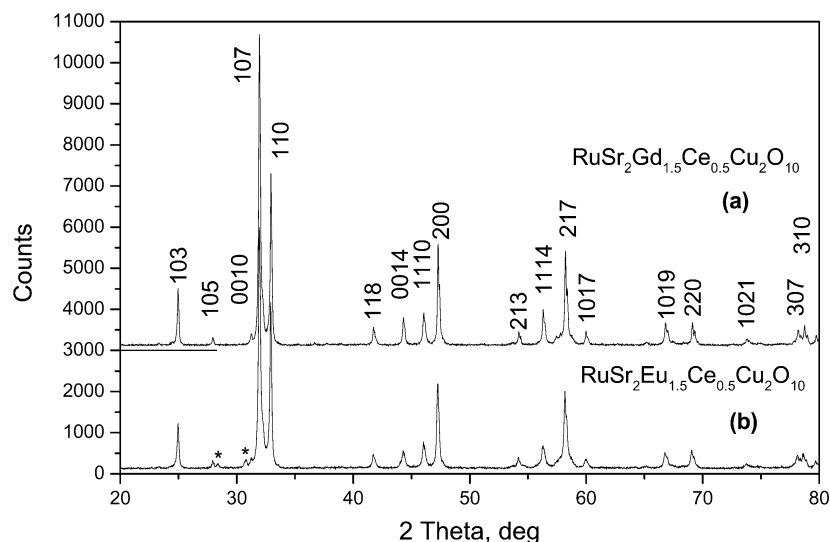


**Figure 1.** XRD patterns of (a)  $\text{RuSr}_2\text{Gd}_{1.5}\text{Ce}_{0.5}\text{Cu}_2\text{O}_{10}$  and (b)  $\text{RuSr}_2\text{Eu}_{1.5}\text{Ce}_{0.5}\text{Cu}_2\text{O}_{10}$ . Asterisks mark impurity peaks.

Electron diffraction patterns were obtained using a JEOL-200EX TEM operated at 200 kV with a double-tilt holder. The electron beam was well aligned and camera length was refined using four diffraction rings from the thin Au film deposited onto the microgrid. Thus-obtained values of camera length were applied for diffraction patterns indexing. To prepare the samples for TEM studies, the pieces of specimens were carefully grinded under absolute methanol. After sedimentation, a drop was transferred onto the Cu grid covered by holey carbon film and left under ambient conditions for methanol evaporation. High-resolution lattice images of the same thin crystals fragments with the additional diffraction spots along  $00l$  direction were taken by Hitachi HF-2200 TEM at 200 kV for the  $[010]$  electron beam incidence. After the HREM image recording the chemical composition of the particles was confirmed by the EDX.

Raman spectra were excited with the 514.5-nm line of an Ar ion laser and measured at room temperature in a back-scattering geometry using microprobe optics (designed by Atago-Bussan Co. Ltd.). The incident laser beam with a power of  $\sim 1$  mW was focused onto the sample surface to a spot of about  $2\text{--}3$   $\mu\text{m}$  using a  $\times 90$  long-working distance lens. The Raman spectra were taken using a Jobin-Yvon T64000 system with a liquid nitrogen-cooled CCD detector. We used a single spectrograph, equipped with 600 grooves/mm diffraction grating, eliminating the laser line with a holographic notch filter (Super Notch Filter, Kaiser Optics Co. Ltd.). Typical exposure time of a CCD camera was 5 min. The prepared pellets were broken and the spectra were collected from the fresh surface. At least five grains were checked to obtain representative data.

## Results and Discussion

The XRD pattern presented in Figure 1a corresponds to single phase of  $\text{RuSr}_2\text{Gd}_{1.5}\text{Ce}_{0.5}\text{Cu}_2\text{O}_{10}$  ( $I4/mmm$ ,  $a = 3.8381(2)\text{\AA}$  and  $c = 28.578(1)\text{\AA}$ ). Occasionally examination of similar samples by SEM (Hitachi model S-4500 equipped with EDS detector and QUASAR–Kevex software for quantitative microanalysis) may reveal the presence of an impurity phase –  $\text{SrRuO}_3$  possibly doped with Gd. However, the amount of  $\text{SrRuO}_3$  refined by the Rietveld method in such samples does not exceed 3 wt % (for the sample in Figure 1a it was 2.3 wt %). According to our experience, the presence of  $\text{SrRuO}_3$  indicates the excess of ruthenium oxide (or high  $P_{\text{RuO}_3}$ ) in the starting composition. 10–15% of  $\text{SrRuO}_3$  also forms if the temperature of syntheses exceeds  $1080$   $^\circ\text{C}$ . In the latter case, it can be easily distinguished by SEM-EDS on the faces of crystallites in the form of drops

solidified from Cu-rich flux. The Ru deficient starting composition, on the other hand, usually yields  $\text{Sr}_2\text{GdRuO}_6$  as the main impurity. Synthesis of  $\text{RuSr}_2\text{Eu}_{1.5}\text{Ce}_{0.5}\text{Cu}_2\text{O}_{10}$  is more difficult than the Gd case. The major phase is accompanied usually by an impurity that has strong reflections in the range of  $2\theta$   $28.3\text{--}28.4$  and  $30.6\text{--}30.9^\circ$ , which in Figure 1b are pointed out by the asterisks. This compound does not have a good match in the PDF database and the presence of only a few peaks does not allow identification of its lattice parameters. According to the EDS data, this phase has an approximate chemical composition of  $\text{Sr}_{1.55}\text{Eu}_{1.25}\text{Ce}_{0.2}\text{Ru}_{0.8}\text{Cu}_{0.2}\text{O}_6$ , which should be isostructural to  $\text{Sr}_2\text{GdRuO}_6$  and cannot be responsible for superconductivity. The rest of the diffraction peaks correspond to the  $\text{RuSr}_2\text{Eu}_{1.5}\text{Ce}_{0.5}\text{Cu}_2\text{O}_{10}$  ( $I4/mmm$ ,  $a = 3.8401(3)\text{\AA}$  and  $c = 28.5597(20)\text{\AA}$ ). The difficulty of obtaining a  $\text{RuSr}_2\text{Eu}_{1.5}\text{Ce}_{0.5}\text{Cu}_2\text{O}_{10}$  sample of better purity is likely related to the substitution of Eu onto the Sr site, which changes the stoichiometry of the major phase. Although  $\text{Eu}^{3+}$  is almost identical to  $\text{Gd}^{3+}$ , the  $\text{Eu}^{2+}$  ionic radius is very close to the ionic radius of  $\text{Sr}^{2+}$ . We must emphasize that samples of exceptional quality can be synthesized; nevertheless, in this study we intentionally used samples prepared under identical conditions in the same series with the Ru-deficient samples. The Ru deficient sample in this study was the same as that in our previous work,<sup>13</sup> having bulk chemical composition of  $\text{Ru}_{0.9}\text{Sr}_2\text{Eu}_{1.5}\text{Ce}_{0.5}\text{Cu}_2\text{O}_{10}$  ( $a = 3.8407(4)\text{\AA}$ ,  $c = 28.543(3)\text{\AA}$ ).

Figure 2 shows that absence of superconductivity is not a unique property of the  $\text{RuSr}_2\text{Eu}_{1.5}\text{Ce}_{0.5}\text{Cu}_2\text{O}_{10}$  ceramics. Both  $\text{RuSr}_2\text{Ln}_{1.5}\text{Ce}_{0.5}\text{Cu}_2\text{O}_{10}$  compounds with  $\text{Ln} = \text{Gd}$  and  $\text{Ln} = \text{Eu}$  demonstrate semiconducting type of resistivity vs temperature dependence which changes at  $\sim 35\text{--}40$  K, however samples do not become bulk superconductors even at 4 K. The resistivity data and magnetic susceptibility data<sup>13</sup> made us suspect that Ru-1222 intrinsically is not a superconducting compound, and that superconductivity appears as a result of the divergence of the cation stoichiometry, for instance, due to ruthenium oxide loss during the solid-state reaction. In fact, the resistivity data in Figure 2, plotted for Ru deficient starting composition ( $\text{Ru}_{0.9}\text{Sr}_2\text{Eu}_{1.5}\text{Ce}_{0.5}\text{Cu}_2\text{O}_{10}$ ) is quite typical for high  $T_c$  materials. The magnetic

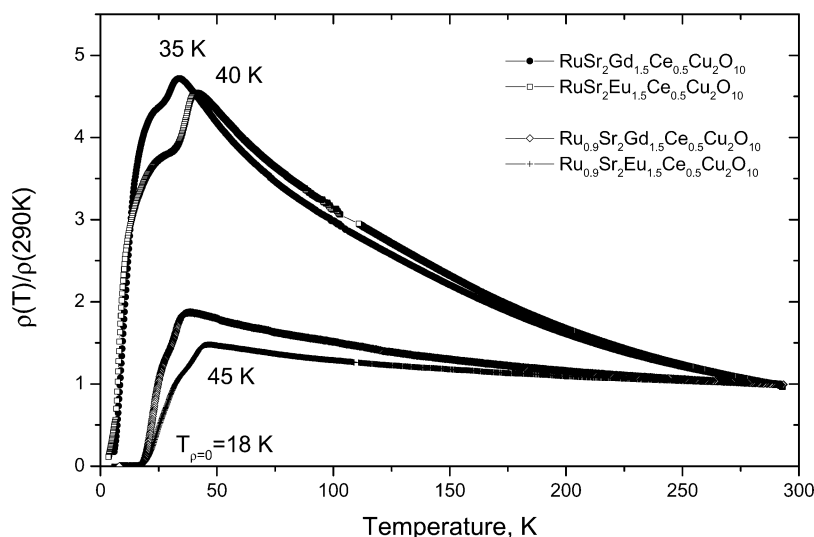


**Figure 2.** Resistivity vs temperature data of (●)  $\text{RuSr}_2\text{Gd}_{1.5}\text{Ce}_{0.5}\text{Cu}_2\text{O}_{10}$ , (□)  $\text{RuSr}_2\text{Eu}_{1.5}\text{Ce}_{0.5}\text{Cu}_2\text{O}_{10}$ , (◇)  $\text{Ru}_{0.9}\text{Sr}_2\text{Gd}_{1.5}\text{Ce}_{0.5}\text{Cu}_2\text{O}_{10}$ , and (+)  $\text{Ru}_{0.9}\text{Sr}_2\text{Eu}_{1.5}\text{Ce}_{0.5}\text{Cu}_2\text{O}_{10}$ . The data were normalized by the resistivity at  $T = 290$  K.

susceptibility data for the synthesized samples demonstrate history dependence common for ferromagnetic materials (see Supporting Information) with the irreversibility temperature of approximately 180 K for both Ln = Gd and Eu. Magnetic shielding by the superconducting phase manifests only for the sample of  $\text{Ru}_{0.9}\text{Sr}_2\text{Eu}_{1.5}\text{Ce}_{0.5}\text{Cu}_2\text{O}_{10}$  bulk composition; however, the volume fraction of the superconducting phase is of the order of 1%. The accurate estimation of superconducting volume fraction in those samples is difficult because of the ferromagnetic contribution from Ru-1222 and multiphase nature of superconducting ceramic specimens. Even if one would assume that the decrease of susceptibility below  $T_C$  for the zero field cooled curve is only due to the magnetic screening, it would give the estimation of the superconducting phase volume fraction of the order of 10%. We have never observed the bulk Meissner effect for our samples.

To find the difference responsible for the appearance of superconductivity we have carried out more careful characterization of  $\text{RuSr}_2\text{Eu}_{1.5}\text{Ce}_{0.5}\text{Cu}_2\text{O}_{10}$  and  $\text{Ru}_{0.9}\text{Sr}_2\text{Eu}_{1.5}\text{Ce}_{0.5}\text{Cu}_2\text{O}_{10}$  samples by TEM and electron diffraction. The selected area electron diffraction pattern of the nonsuperconducting stoichiometric sample for [010] incident beam in Figure 3a does not contain any unexpected features for  $I4/mmm$  space group—the distance between diffraction spots corresponds well to the lattice parameters obtained from the XRD data, and the  $h + k + l = 2n$  limiting condition is fulfilled.

The electron diffraction pattern of the superconducting sample of  $\text{Ru}_{0.9}\text{Sr}_2\text{Eu}_{1.5}\text{Ce}_{0.5}\text{Cu}_2\text{O}_{10}$  bulk composition in Figure 3b contains diffuse scattering along  $00l$  direction and diffraction spots resembling  $h0l$  ( $h + 1 = 2n + 1$ ) peaks, which should not appear for the  $I4/mmm$  space group. Both features imply a presence of disorder in the structure. More detailed analysis of the enlarged pattern (Figure 3c) shows that single crystal-like grains contain a second phase, which epitaxially forms within Ru-1222 structure, and its lattice parameters can be expressed through Ru-1222 lattice parameters as follows:  $\mathbf{a} = \mathbf{a}_{\text{Ru-1222}}$ ,  $\mathbf{c} = \frac{2}{5}\mathbf{c}_{\text{Ru-1222}}$ . The diffraction spots in Figure 3c correspond to  $d_{002} = 14.56$  Å of Ru-1222 and  $d'_{001} = 11.44$  Å for the satellite phase. The HREM

image of the  $\text{Ru}_{0.9}\text{Sr}_2\text{Eu}_{1.5}\text{Ce}_{0.5}\text{Cu}_2\text{O}_{10}$  particle aligned along the same zone axis in Figure 3d demonstrates an intergrowth of the parasitic phase with the simpler layered structure in the main Ru-1222 compound. Using Ru-1222 lattice as a reference we can estimate the  $\mathbf{c}$  axis of the satellite phase in the HREM image as approximately 11.45 Å. Taking lattice parameters of Ru-1222 determined from the XRD pattern of the sample and the obtained relationship  $\mathbf{a} = \mathbf{a}_{\text{Ru-1222}}$ ,  $\mathbf{c} = \frac{2}{5}\mathbf{c}_{\text{Ru-1222}}$ , we can estimate lattice parameters of the parasitic epitaxial phase more precisely:  $\mathbf{a} = 3.8407$  Å,  $\mathbf{c} = 11.417$  Å. The closest results from the ICSD search include only  $\text{YSr}_2\text{Cu}_3\text{O}_7$  and  $\text{YSr}_2\text{Cu}_{3-x}\text{M}_x\text{O}_{7+z}$  compounds where M = Co, Fe, Ga, or Mo with various degrees of substitution. The  $\mathbf{c}/\mathbf{a}$  ratio of 2.97 also suggests triple perovskite as the likely candidate for this epitaxial phase. Note, lattice parameters of  $\text{RuSr}_2\text{EuCu}_2\text{O}_8$  are 3.842 Å and 11.577 Å, and therefore intergrowth of such a phase in the pure form cannot explain adequately lattice parameters of the parasitic phase. Thus, we concluded that the most probable parasitic phase is  $\text{EuSr}_2\text{Cu}_{3-x}\text{Ru}_x\text{O}_{7+z}$  solid solution with a small degree of substitution (small  $x$ ).

To verify this hypothesis we have collected Raman spectra excited with the 514.5 nm line of an Ar ion laser. With respect to Raman spectra, the samples looked homogeneous and all the collected spectra were similar to those shown in Figure 4. We assumed that if the satellite phase of  $\text{EuSr}_2\text{Cu}_{3-x}\text{Ru}_x\text{O}_{7+z}$  was present in a reasonable amount, which may explain bulk superconductivity, we should be able to see its signature by the appearance of an apical oxygen mode in the region similar to  $\text{YSr}_2\text{Cu}_3\text{O}_7$  compounds at approximately 550  $\text{cm}^{-1}$ <sup>14</sup> and its frequency will be significantly different from the apical oxygen mode in the Ru-1222 or Ru-1212 typically located at 650  $\text{cm}^{-1}$ <sup>15,16</sup> where an oxygen atom is confined between copper and Ru atoms. Figure 4a presents Raman spectra of a nonsuperconducting sample

(14) Lee, H.-G.; Litvinchuk, A. P.; Abrashev, M. V.; Iliev, M. N.; Xu, S. H.; Chu, C. W. *J. Phys. Chem. Solids* **1998**, *59*, 1994.

(15) Fainstein, A.; Pregeliasco, R. G.; Williams, G. V. M.; Trodahl, H. J. *Phys. Rev. B* **2002**, *65*, 184517-1.

(16) Williams, G. V. M.; Ryan, M. *Phys. Rev. B* **2001**, *64*, 094515-1.

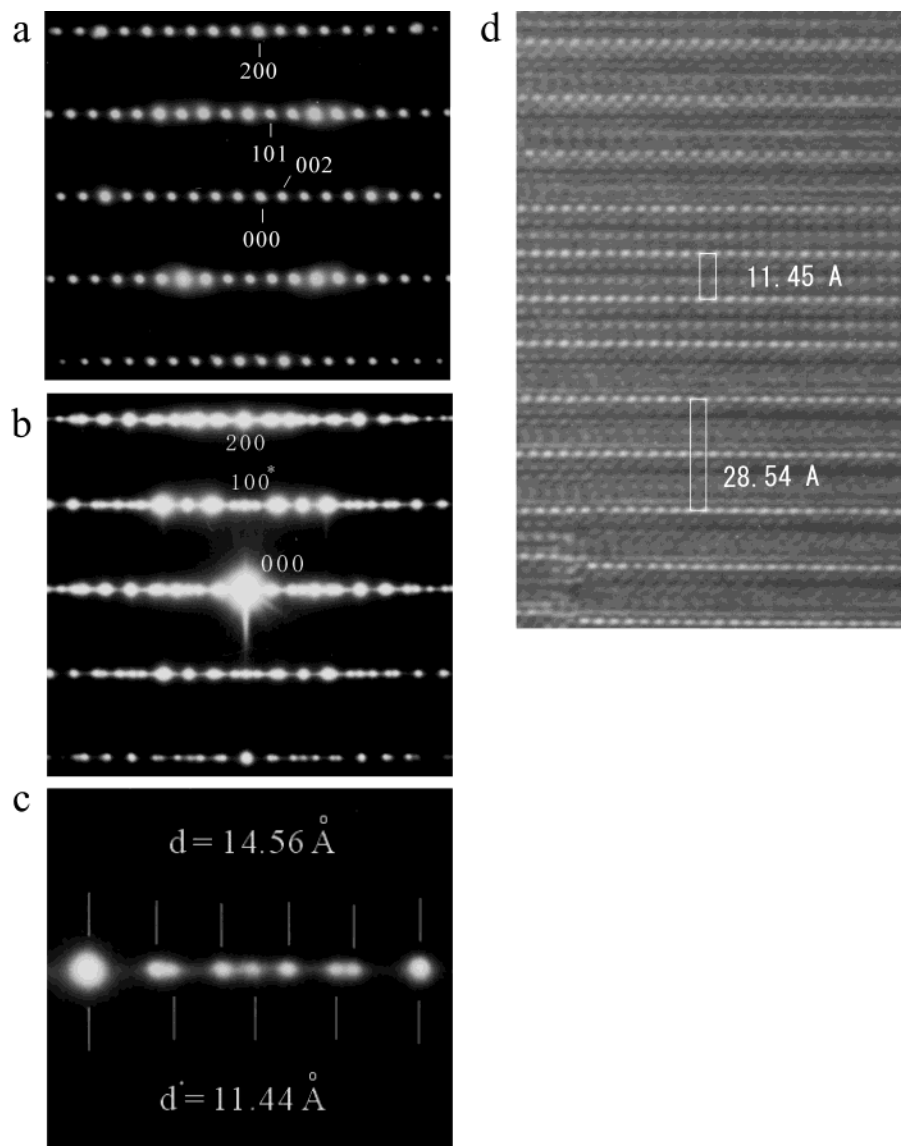


**Figure 3.** Selected area electron diffraction (SAED) pattern for the beam incidence along [010] direction of (a)  $\text{RuSr}_2\text{Eu}_{1.5}\text{Ce}_{0.5}\text{Cu}_2\text{O}_{10}$ ; and (b)  $\text{Ru}_{0.9}\text{Sr}_2\text{Eu}_{1.5}\text{Ce}_{0.5}\text{Cu}_2\text{O}_{10}$  ( $100^*$  reflection is not allowed for  $I4/mmm$  space group). (c) Enlarged region of the  $\text{Ru}_{0.9}\text{Sr}_2\text{Eu}_{1.5}\text{Ce}_{0.5}\text{Cu}_2\text{O}_{10}$  electron diffraction pattern showing coexistence of two phases with reflections corresponding to  $1/2\text{c}_{\text{Ru-1222}}$  and  $2/5\text{c}_{\text{Ru-1222}}$ . (d) HREM lattice image corresponding to the [010] zone axis of  $\text{Ru}_{0.9}\text{Sr}_2\text{Eu}_{1.5}\text{Ce}_{0.5}\text{Cu}_2\text{O}_{10}$ ; the lattice parameter of the satellite phase was estimated using  $\text{Ru}_{0.9}\text{Sr}_2\text{Eu}_{1.5}\text{Ce}_{0.5}\text{Cu}_2\text{O}_{10}$  as a reference.

of  $\text{RuSr}_2\text{Eu}_{1.5}\text{Ce}_{0.5}\text{Cu}_2\text{O}_{10}$ . The spectrum of the nonsuperconducting compound is similar to the reported spectra collected from Ru-1222 grains.<sup>16</sup> The low intensity peaks in our case look less clear probably because of the small particle size and imperfect grain shape in the samples prepared by sol-gel method. The Raman spectrum in Figure 4b corresponds to the superconducting sample with  $\text{Ru}_{0.9}\text{Sr}_2\text{Eu}_{1.5}\text{Ce}_{0.5}\text{Cu}_2\text{O}_{10}$  starting composition. One may notice the small increase of a peak at  $540\text{ cm}^{-1}$  that we expected due to the presence of Cu in Ru site; however, the presence of the other peaks at  $757\text{ cm}^{-1}$  and  $1452\text{ cm}^{-1}$ , and a broad band at  $\sim 1100\text{ cm}^{-1}$ , was unexpected. Such modes have not been reported for either Ru-1222 or Ru-1212. Relatively high frequency of two peaks (above  $1000\text{ cm}^{-1}$ ) indicates that the new vibrations do not correspond to the phonons in the oxide material, but more likely originate from intermolecular vibrations in a molecular group. Moreover, the observed frequencies correspond well to the  $\text{CO}_3^{2-}$  group which coordinates a metal ion in the mono-

dentate manner.<sup>17</sup> It is interesting that a fully symmetric mode at  $\sim 1000\text{--}1100\text{ cm}^{-1}$ , which is well pronounced in the alkaline-earth carbonates, has very low intensity in our superconducting Ru-1222 sample, therefore we may conclude that  $\text{SrCO}_3$  cannot be an explanation of  $\text{CO}_3^{2-}$  group presence on one hand, and, on the other hand, carbonate group should be bridging Cu atoms similar to  $\text{CO}_3^{2-}$  group in  $\text{Ba}_4\text{CaCu}_2\text{O}_{6+d}(\text{CO}_3)$ ,<sup>18</sup>  $\text{Ba}_{1.5}\text{Sr}_{0.5}\text{CuO}_{3+d}(\text{CO}_3)_y$ ,<sup>19</sup> or  $\text{Sr}_2\text{CuO}_2(\text{CO}_3)$ .<sup>20</sup> The last compound itself could not be responsible for the observed spectrum because it has a strong phonon mode at  $500\text{ cm}^{-1}$  and a strong broad band at  $\sim 1200\text{ cm}^{-1}$ ,

(17) Nakamoto, K. *Infrared and Raman spectra of Inorganic and Coordination Compounds*, A Wiley-Interscience Publication; John Wiley and Sons: New York, 1978.

(18) Kikuchi, M.; Izumi, F.; Kikuchi, M.; Ohshima, E.; Morii, Y.; Shimojo, Y.; Syono, Y. *Physica C* **1995**, *247*, 183.

(19) Mertelj, T.; Mateev, D.; Maticcotta, F. C.; Pal, D.; Stastny, P.; Nozar, P.; Jiang, Q. *Solid State Commun.* **1992**, *84*, 1115.

(20) Nakata, H.; Akimitsu, J.; Katano, S.; Minami, T.; Ogita, N.; Udagawa, M. *Physica C* **1995**, *255*, 157.

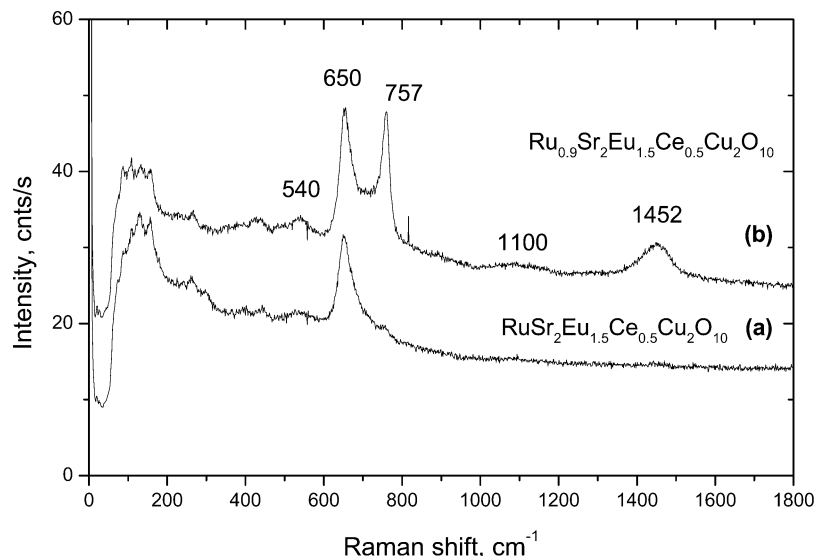


**Figure 4.** Micro-Raman spectra of (a) nonsuperconducting  $\text{RuSr}_2\text{Eu}_{1.5}\text{Ce}_{0.5}\text{Cu}_2\text{O}_{10}$  and (b) superconducting  $\text{Ru}_{0.9}\text{Sr}_2\text{Eu}_{1.5}\text{Ce}_{0.5}\text{Cu}_2\text{O}_{10}$  materials.

while the mode at  $1450\text{ cm}^{-1}$  is extremely weak or even completely absent.

Thus, according to the electron diffraction data, the superconducting sample of Ru-1222 ceramics contains an epitaxial satellite phase with the triple perovskite structure and lattice parameters corresponding to  $\text{EuSr}_2\text{Cu}_{3-x}\text{Ru}_x\text{O}_{7+z}$  ( $x$  is small), and according to Raman spectroscopic data collected from the crystalline grains, it contains  $\text{CO}_3^{2-}$  bridging groups. On the basis of those facts we speculate that the composition of the parasitic epitaxial phase is  $\text{EuSr}_2\text{Cu}_{3-x}(\text{CO}_3)_x\text{O}_{7+z}$  likely doped with Ru into the Cu chain site. At the moment we do not have solid data on the exact chemical composition of this phase and its structure, however profound studies are currently in progress. We would like to stress that even though high- $T_c$  carboxycuprates were regarded as an elegant idea or a game of mind about 10 years ago, their existence becomes evident after synthesis of  $(\text{C}_{0.4}\text{Cu}_{0.6})\text{Sr}_2(\text{Y}_{0.86}\text{Sr}_{0.14})\text{Cu}_2\text{O}_7$ ,<sup>21</sup>  $(\text{Ba}_{1-x}\text{Sr}_x)_2\text{Cu}_{1+y}\text{O}_{2+2y+z}(\text{CO}_3)_{1-y}$ ,<sup>22</sup>  $\text{Y}_{1.6}\text{Ca}_{0.4}\text{Ba}_4\text{Cu}_5\text{O}_{11}(\text{CO}_3)$ ,<sup>23</sup> and other superconducting carboxycuprates.

We were surprised to find  $\text{CO}_3^{2-}$  vibrations in the Raman spectra of our superconducting Ru-1222 ceramics because we made special efforts to exclude inhomogeneity by use of highly homogeneous precursors, and to remove carbonates by conducting annealing in the dynamic vacuum and in the oxygen flow. Note that all of the studies on the Ru-1222 cited in this report make use of conventional ceramic methods, take  $\text{SrCO}_3$  as a starting reagent for the synthesis, and do not check the presence of  $\text{CO}_3^{2-}$  groups in the lattice. In general, high valence cation doping into the copper chain site is required to stabilize the  $\text{YSr}_2\text{Cu}_3\text{O}_7$  phase under normal pressure.<sup>24</sup> Although without doping it can be prepared only at high pressure, we should not exclude that in our particular case it may form under normal pressure due to the epitaxy on the suitable substrate, Ru-1222, or due

to doping by a carbonate group into the chain site. The superconducting transition in carbon-free  $\text{YSr}_2\text{Cu}_3\text{O}_7$  occurs at  $T_c = 60\text{ K}$ ,<sup>25</sup> which is rather high compared to the  $T_c$  of Ru-1222 samples. However, according to Akimitsu et al.<sup>26</sup>  $(\text{Y}_{0.5}\text{Ca}_{0.5})_{0.95}\text{Sr}_{2.05}\text{Cu}_{2.4}(\text{CO}_3)_{0.6}\text{O}_y$  reached zero resistivity at 38 K. More interesting fact is that such a compound was obtained at  $1050\text{ }^\circ\text{C}$  – the optimal temperature for synthesis of Ru-1222. Although calcium is absent in our system, we should also expect lower  $\text{CO}_3^{2-}$  concentration because of lower  $\text{CO}_2$  partial pressure in our synthesis procedure. The conclusion about low  $\text{CO}_3^{2-}$  content can be made considering longer  $c$ -axis in the satellite phase compared to  $(\text{Y}_{0.5}\text{Ca}_{0.5})_{0.95}\text{Sr}_{2.05}\text{Cu}_{2.4}(\text{CO}_3)_{0.6}\text{O}_y$ . In such a case one may anticipate the value of  $T_c$  equal to 20–40 K also for the observed satellite compound. Of course, our observation of the intergrowth of an oxocarbonate in Ru-1222 may be restricted to only the specific synthetic method, though the formation of  $\text{EuSr}_2\text{Cu}_{3-x}(\text{CO}_3)_x\text{O}_{7+z}$  epitaxial parasitic phase in our Ru-1222 ceramics might be a good hint for explanation of superconductivity and ferromagnetism appearance in this material. Although Yang et al.<sup>27</sup> have also reported observation of metastable superstructures in the  $\text{RuSr}_2\text{Gd}_{1.4}\text{Ce}_{0.6}\text{Cu}_2\text{O}_{10}$  samples prepared by conventional ceramic method, it is difficult to make a direct comparison between the samples because conventional Ru-1222 specimens seem to have a more abundant set of superstructures. We believe that more profound investigation of Ru-1222 real structure is necessary to have an adequate view of the solid-state chemistry and physics of this material. Taking into account possible variable oxygen concentration in the satellite phase one may expect quite broad range of  $T_c$  for superconducting Ru-1222 ceramic samples. However oxygen nonstoichiometry might be restricted by the lattice matching between Ru-1222 and the parasitic phase because change of  $\text{EuSr}_2\text{Cu}_{3-x}(\text{CO}_3)_x\text{O}_{7+z}$  lattice

(21) Miyazaki, Y.; Yamane, H.; Ohnishi, N.; Kajitani, T.; Hiraga, K.; Morii, Y.; Funahashi, S.; Hirai, T. *Physica C* **1992**, *198*, 7.

(22) Kinoshita, K.; Yamada, T. *Nature* **1992**, *357*, 313.

(23) Hervieu, M.; Boullay, Ph.; Domenges, B.; Maignan, A.; Raveau, B. *J. Solid State Chem.* **1993**, *105*, 300.

(24) Den, T.; Kobayashi, T. *Physica C* **1992**, *196*, 141.

(25) Okai, B. *Jpn. J. Appl. Phys. Part 2* **1990**, *29*, L2180.

(26) Akimitsu, J.; Uehara, M.; Ogawa, M.; Nakata, H.; Tomimoto, K.; Miyazaki, Y.; Yamane, H.; Hirai, T.; Kinoshita, K.; Matsui, Y. *Physica C* **1992**, *201*, 320.

(27) Yang, L.; Viera, J. M.; Tang, K.; Zhou, G. *Mater. Res. Soc. Symp. Proc.* **2002**, *689*, E 4.7.1.

parameters upon oxidation or reduction should increase strain due to the lattices mismatch.

In conclusion, we should emphasize that extremely long synthesis or use of high oxygen pressure for preparation of superconducting Ru-1222 ceramics are the conditions which favor gradual ruthenium oxide escape from the sample<sup>28</sup> and formation of  $\text{EuSr}_2\text{Cu}_{3-x}(\text{CO}_3)_x\text{O}_{7+z}$  superconducting layers. We would like to note that a conclusion about coexistence of superconducting  $\text{EuSr}_2\text{Cu}_{3-x}(\text{CO}_3)_x\text{O}_{7+z}$  and intrinsically ferromagnetic  $\text{RuSr}_2\text{Eu}_{1.5}\text{Ce}_{0.5}\text{Cu}_2\text{O}_{10}$  compounds in the Ru-1222 ceramics is consistent with the recent profound

studies of the electrical and magnetic properties carried out by Xue et al.<sup>11</sup> who have found that superconductivity and ferromagnetism possibly appear as a result of the phase separation and, in addition, the volume fraction of the Meissner phase is small.

**Acknowledgment.** This work was financially supported by Grant-in-Aid for Scientific Research 13001266.

**Supporting Information Available:** Magnetic susceptibility data for the superconducting and nonsuperconducting  $\text{RuSr}_2\text{Ln}_{1.5}\text{Ce}_{0.5}\text{Cu}_2\text{O}_{10}$  (Ln = Eu and Gd) samples discussed in the paper. This material is available free of charge via the Internet at <http://pubs.acs.org>.

---

(28) Bell, W. E.; Tagami, M. *J. Phys. Chem.* **1963**, *67*, 2432.